

Supporting Information

Defect engineering in two-dimensional perovskite nanowire arrays by Europium (III) doping towards high-performance photodetection

Yuwei Guan, Jie Liang, Yiman Zhao, Zhen Liu, Zhonghao Zhou, Shiyang Ji, Yajun Jia, Fengqin Hu, and Yong Sheng Zhao**

[†]College of Chemistry, Beijing Normal University, Beijing 100875, China

[‡]Key Laboratory of Photochemistry, Institute of Chemistry, Chinese Academy of Sciences, Beijing 100190, China.

Corresponding authors: *fqhu@bnu.edu.cn; *yszha@iccas.ac.cn

Contents

- i. **Experimental details.**
 - 1). Materials.
 - 2). Preparation of the undoped and the Eu-doped $(\text{PEA})_2\text{PbI}_4$ crystals:
 - 3). Preparation of the undoped and the Eu-doped $(\text{PEA})_2\text{PbI}_4$ nanowire arrays
 - 4). Characterizations.
 - 5). Device fabrication.
 - 6). Detector performance measurements.
- ii. **Fig. S1.** Schematic illustration of the preparation of the undoped and the Eu-doped $(\text{PEA})_2\text{PbI}_4$ nanowire arrays.
- iii. **Fig. S2.** The morphology of the 3% and 9% Eu-doped $(\text{PEA})_2\text{PbI}_4$ nanowire arrays.
- iv. **Fig. S3.** The energy dispersive X-ray spectroscopy (EDS) mappings on the 3% Eu-doped $(\text{PEA})_2\text{PbI}_4$ nanowires.
- v. **Fig. S4.** Tauc plots of the undoped and the Eu-doped $(\text{PEA})_2\text{PbI}_4$ nanowire arrays.
- vi. **Fig. S5.** Time-resolved photoluminescence (TRPL) of the undoped and Eu-doped PEA_2PbI_4 nanowire arrays.
- vii. **Table.S1.** The calculated values of the carrier lifetimes (τ_1 and τ_2).
- viii. **Fig. S6.** Schematic illustration of the fabrication of the photodetectors based on the undoped and the Eu-doped $(\text{PEA})_2\text{PbI}_4$ nanowire arrays.
- ix. **Fig. S7.** Schematic illustration of a home-built two-probe micro-photoelectric testing system.
- x. **Fig. S8.** Light-intensity-dependent current densities of the photodetectors based on the undoped and 6% Eu-doped $(\text{PEA})_2\text{PbI}_4$ nanowire arrays.
- xi. **Fig. S9.** Light-intensity-dependent specific detectivities of the photodetectors based on the undoped and 6% Eu-doped $(\text{PEA})_2\text{PbI}_4$ nanowire arrays.
- xii. **Fig. S10.** $I-t$ response of the photodetectors under 532 nm illumination of the same irradiance (0.70 mW/cm^2).
- xiii. **Fig. S11.** $I-t$ response of the photodetectors based on the 6% Eu-doped $(\text{PEA})_2\text{PbI}_4$ nanowire arrays after 30 days.

Experimental details

Materials: 2-Phenylethylamine (PEA, 99%, optical purity > 97%), Lead (II) acetate trihydrate (99.5%) and 55-57% aqueous hydriodic acid (HI) solution were purchased from Innochem Science & Technology (Beijing, China). N, N-anhydrous dimethylformamide (DMF), anhydrous dimethyl sulfoxide (DMSO), were purchased from J&K Chemical.

Preparation of the undoped and the Eu-doped (PEA)₂PbI₄ crystals: The synthesis of the CHP single crystals was adapted from literature reports.^{1, 2} First, 0.379 g of (CH₃COO)₂Pb (1 mmol), 0.242 g (2 mmol) of PEA, and 10 ml of 57% hydrogen iodide (HI) solution were loaded into a glass vial. The formed yellow precipitates were subsequently dissolved at 130 °C. The reaction stock solution was then cooled to room temperature under ambient conditions, resulting in the formation of orange flake-like crystals. These crystals were vacuum-filtrated and rinsed with toluene several times. Finally, the crystals were dried in vacuum overnight.

Preparation of the undoped and the Eu-doped (PEA)₂PbI₄ nanowire arrays: The Si/SiO₂ substrates were washed by deionized water and alcohol for several times. Then, the substrates were processed in plasma cleaner for 6 minutes. The precursor solutions were prepared by directly dissolving synthesized bulk crystals into a mixed solvent of DMF and DMSO (the volume ratio is 1:1). A “capillary-bridge rise” assembly system was constructed by combining an asymmetric-wettability topographical template and a target substrate. The assembly system was contacted with the solutions of precursor for a few seconds. The precursor liquid will rise in the gaps between the top of micropillars and substrate driven by capillary force and Laplace pressure, and then forming individual capillary bridges anchored onto the top of the micropillars. The assembly system was moved away from precursor liquid and heated at 80 °C for 20 hours to realize the total evaporation of DMF and DMSO solvents. At last, the single-crystalline nanowires were generated onto target substrates after detaching the micropillar template.³

Characterization: The morphology and crystallinity of the nanowire arrays were examined by scanning electron microscopy (SEM, Hitachi S-4800). Fluorescence micrographs were taken with an inverted fluorescence microscope (Nikon Ti-U) equipped with a high-resolution color digital camera (DS-Ri1). The crystal structure of the as-prepared CHP powders and arrays were characterized by X-ray diffraction (XRD, Japan Rigaku D/max-2500) with Cu K α radiation ($\lambda = 0.154$ nm). The UV-vis absorption and photoluminescence (PL) spectra were measured with a Shimadzu UV-2600 spectrophotometer and spectrometer equipped with a 600 gr/mm grating excited by a 405 nm

continuous-wave (CW) laser, respectively. PL lifetime measurements of the nanowire arrays were performed on a Quantaaurus-Tau compact fluorescence lifetime spectrometer (Hamamatsu Photonics, C11367-31, Quantaaurus-Tau, Japan).

Device fabrication: 80 nm Au was deposited by thermal evaporation with a specific metal mask. The channel length and width were controlled to be 50 μm and 500 μm , respectively.

Detector performance measurements: The current-voltage (I - V) measurements were carried out using a Keithley 4200 semiconductor characterization system and a two-probe system at room temperature. The power of the laser was measured with a power meter.

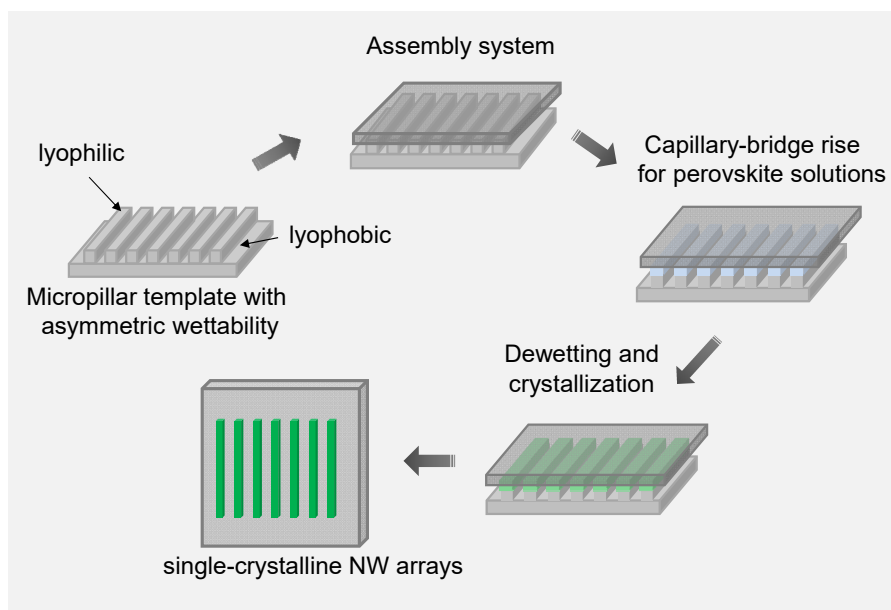


Fig. S1. Schematic illustration of the preparation of the undoped and the Eu-doped $(\text{PEA})_2\text{PbI}_4$ nanowire arrays

The precursor solutions were prepared by dissolving crystals into a mixed solvent of DMF and DMSO (the volume ratio is 1:1). A “capillary-bridge rise” assembly system was constructed by combining an asymmetric-wettability topographical template and the Si/SiO₂ substrate. The assembly system was contacted with the precursor solutions for a few seconds. The precursor liquid will rise in the gaps between the top of micropillars and substrate driven by capillary force and Laplace pressure. Then, the existing individual capillary bridges are anchored onto the top of the micropillars. The assembly system was moved away from precursor solution and heated at 80 °C for 20 hours to realize the total evaporation of solvents. At last, the single-crystalline nanowires were generated onto target substrates after detaching the micropillar template.

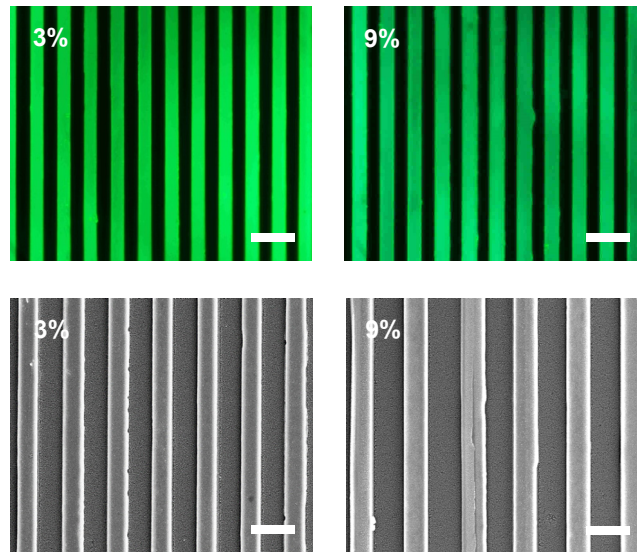


Fig. S2. The morphology of the 3% and 9% Eu-doped $(\text{PEA})_2\text{PbI}_4$ nanowire arrays. Scale bar: 10 μm .

As shown in Fig. S2a-b, the fluorescence microscopy images of the 3% and 9% Eu-doped $(\text{PEA})_2\text{PbI}_4$ nanowire arrays with bright green emissions under UV light irradiation, indicating their homogeneity and uniformity. The scanning electron microscopy (SEM) images in Fig. S2c-d signify the 3% and 9% $(\text{PEA})_2\text{PbI}_4$ nanowire arrays with well-shaped borders and smooth surfaces.

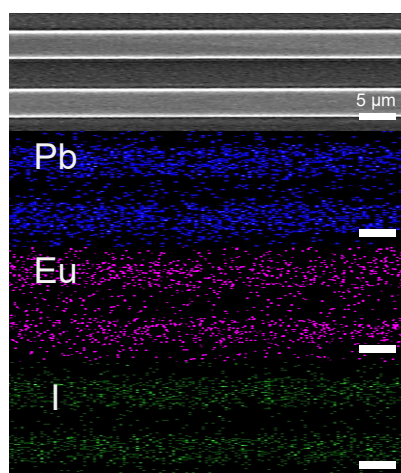


Fig. S3. The energy dispersive X-ray spectroscopy (EDS) mappings on the 3% Eu-doped (PEA)₂PbI₄ nanowires.

The EDS mappings on the 3% Eu-doped nanowires show that europium and other elements are homogeneously dispersed among the whole (PEA)₂PbI₄ nanowires, indicating the successful doping of Eu.

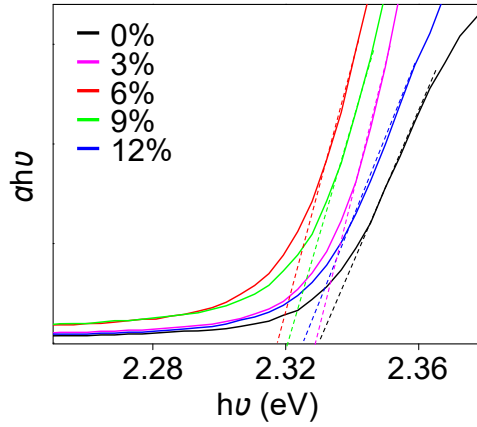


Fig. S4. The Tauc plots of the undoped and Eu-doped PEA₂PbI₄.

Based on the absorption spectra, the bandgaps of the undoped and Eu-doped PEA₂PbI₄ can be calculated by using the equation:

$$(\alpha h\nu)^2 = A(h\nu - E_g)$$

where α and $h\nu$ represent the absorption coefficient and incident photon energy, respectively. The bandgaps of the Eu-doped PEA₂PbI₄ were almost unchanged, indicating that the incorporation of Eu ions didn't introduce deep defect level.

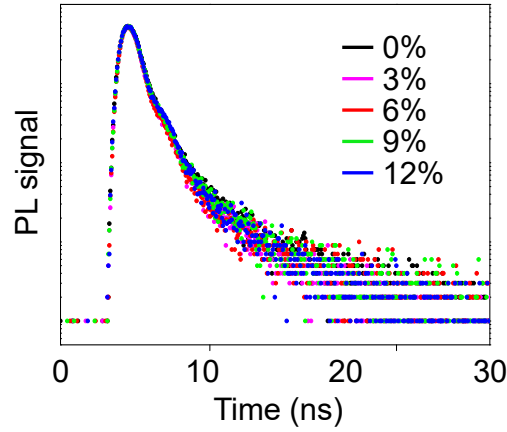


Fig. S5. Time-resolved photoluminescence (TRPL) spectra of the undoped and Eu-doped PEA_2PbI_4 nanowire arrays.

Table S1. The calculated values of the carrier lifetimes (τ_1 and τ_2).

	τ_1 (ns)	τ_2 (ns)
undoped	0.60	2.22
3%	0.51	2.37
6%	0.58	3.16
9%	0.57	2.50
12%	0.45	2.31

The TRPL curves in Fig. S5 are well fitted with a double-exponential decay function, which is defined as:

$$f(t) = A_1 \exp\left(-\frac{t}{\tau_1}\right) + A_2 \exp\left(-\frac{t}{\tau_2}\right) + B$$

The calculated values of carrier lifetime (τ_1 and τ_2) were illustrated in Table S1. The 6% Eu-doped $(\text{PEA})_2\text{PbI}_4$ nanowire arrays exhibit a long fluorescence lifetime ($\tau_2 = 3.16$ ns), which is much longer than the undoped arrays ($\tau_2 = 2.22$ ns). The prolonged fluorescence lifetime can be ascribed to the suppressed non-radiative recombination due to the reduced defect density in the Eu-doped $(\text{PEA})_2\text{PbI}_4$ arrays.

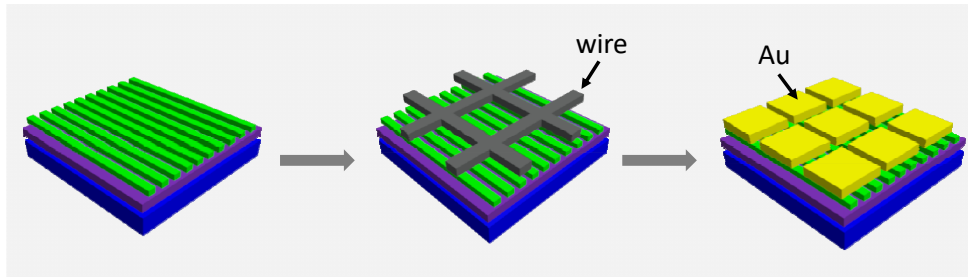


Fig. S6. Schematic illustration of the fabrication of the photodetectors based on the undoped and the Eu-doped $(\text{PEA})_2\text{PbI}_4$ nanowire arrays.

The photodetectors were constructed by depositing Au electrodes on the nanowire arrays assisted with specific metal wires. The thickness of Au electrodes was controlled at 80 nm. The channel length and width were controlled at 50 μm and 500 μm , respectively.

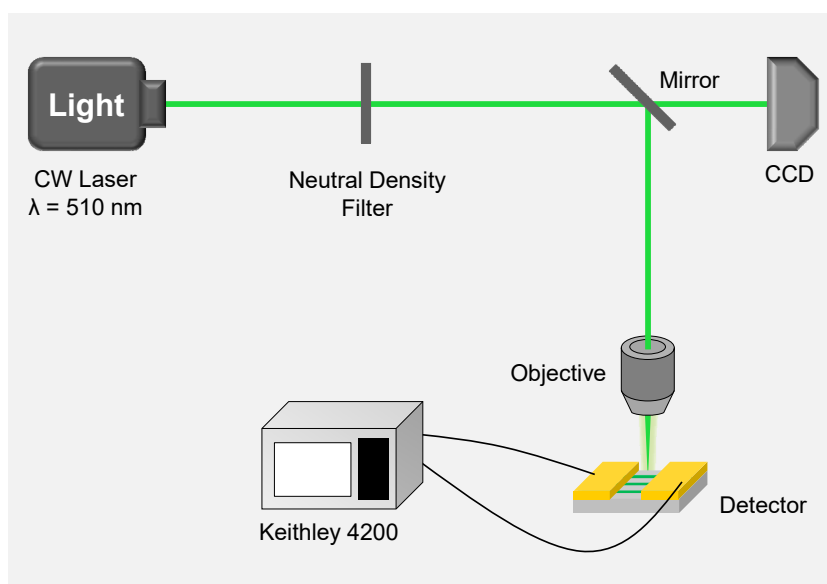


Fig. S7. Schematic illustration of the home-built two-probe micro-photoelectric testing system.

Optoelectronic performance of the devices was measured with a home-built two-probe micro-photoelectric testing system. The continuous-wave lasers ($\lambda = 510 \text{ nm}$) with tunable illumination intensity were used as the light source. The sample on a substrate was excited with the CW laser beam through an objective (Nikon CFLU Plan, 20, N.A. = 0.4), with input power altered by neutral density filters. The I - V characteristics of photodetectors were investigated by using a Keithley 4200 SCS semiconductor parameter analyzer with a two-probe station.

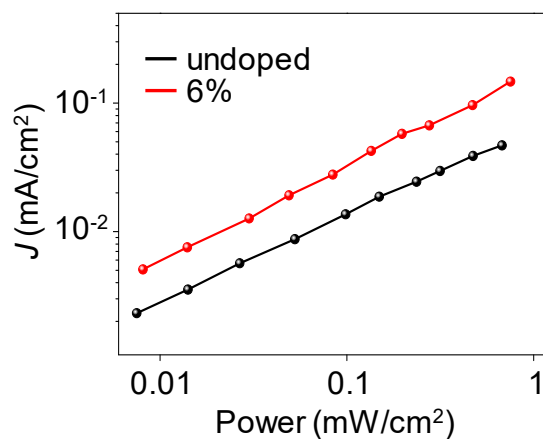


Fig. S8. Light-intensity-dependent current densities (J) of the photodetectors based on the undoped and 6% Eu-doped (PEA)₂PbI₄ nanowire arrays.

Compared with the undoped device, the Eu-doped device exhibits enhanced current density at varying light intensity. The enhanced photoresponse can be attributed to the suppressed trap density in the Eu-doped (PEA)₂PbI₄ nanowire arrays, which facilitates the carrier transport.

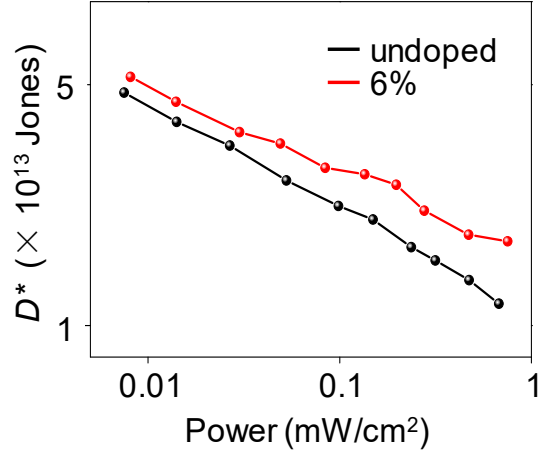


Fig. S9. Light-intensity-dependent specific detectivities (D^*) of the photodetectors based on the undoped and 6% Eu-doped $(\text{PEA})_2\text{PbI}_4$ nanowire arrays.

The specific detectivity (D^*) is calculated by using the equation:

$$D^* = \frac{I_{\text{ph}} \sqrt{S}}{P \sqrt{2eI_{\text{dark}}}}$$

where the e is the elementary charge, I_{ph} is the photocurrent, S is the active area, P is the incident light power, and I_{dark} is the dark current. As shown in Fig. S9, the Eu-doped devices exhibit better detection ability than the undoped devices. The maximum D^* of the Eu-doped devices can reach 5.83×10^{13} , which is equivalent to the 3D perovskite-based perovskites.

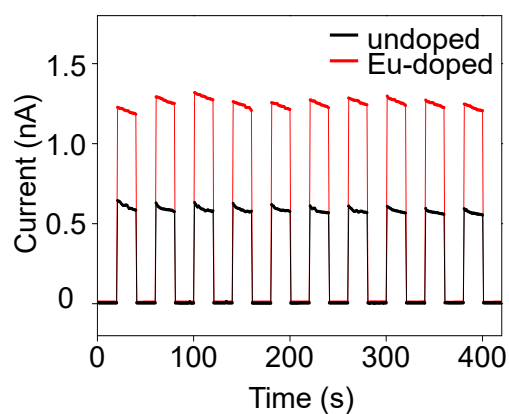


Fig. S10. *I-t* response of the photodetectors under 532 nm illumination of the same irradiance (0.70 mW/cm²).

Besides, 532 nm is also close to the excitonic absorption peak of (PEA)₂PbI₄. We have also investigated the performances of the Eu-doped (PEA)₂PbI₄ photodetector at 532 nm. As shown in Fig. S10, the Eu-doped (PEA)₂PbI₄ photodetector shows superior optoelectronic performance than the undoped (PEA)₂PbI₄ photodetector under 532 nm illumination.

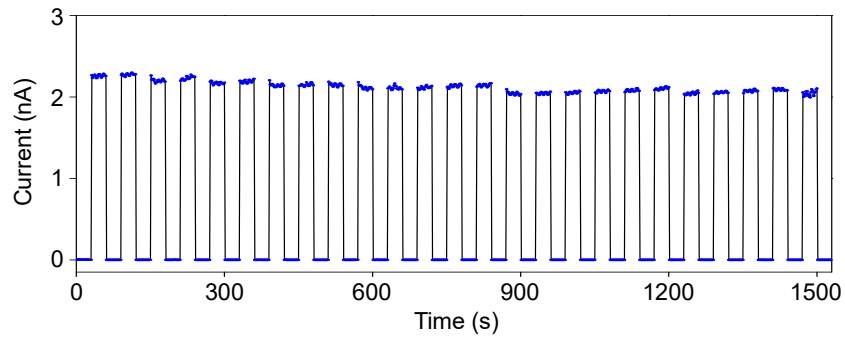


Fig. S11. *I-t* response of the photodetectors based on the 6% Eu-doped $(\text{PEA})_2\text{PbI}_4$ nanowire arrays after 30 days.

After storing in the ambient environment for 30 days, the 6% Eu-doped $(\text{PEA})_2\text{PbI}_4$ photodetectors can maintain over 85% with its initial performance.

References:

1. Y. Dang, X. Liu, Y. Sun, J. Song, W. Hu and X. Tao, *J. Phys. Chem. Lett.*, 2020, **11**, 1689-1696.
2. Z. Liu, C. Zhang, X. Liu, A. Ren, Z. Zhou, C. Qiao, Y. Guan, Y. Fan, F. Hu and Y. S. Zhao, *Adv. Sci.*, 2021, 2102065.
3. J. Feng, C. Gong, H. Gao, W. Wen, Y. Gong, X. Jiang, B. Zhang, Y. Wu, Y. Wu, H. Fu, L. Jiang and X. Zhang, *Nat. Electron.*, 2018, **1**, 404-410.